Experimental Investigations of Quasi-Coherent Micro-Instabilities in J-TEXT Ohmic Plasmas

Peng Shi(石鹏)[1,2], G. Zhuang(庄革)[3], Zhifeng Cheng(程芝峰)[2], Li Gao(高丽)[2], Yinan Zhou(周乙楠)[2], Yong Liu(刘永)[4], J. T. Luo(罗景庭)[4], and Jingchun Li(李景春)[4*]

[1]*Institute of Plasma Physics, Chinese Academy of Sciences, Hefei 230031, China*
[2]*International Joint Research Laboratory of Magnetic Confinement Fusion and Plasma Physics, State Key Laboratory of Advanced Electromagnetic Engineering and Technology, School of Electrical and Electronic Engineering, Huazhong University of Science and Technology, Wuhan 430074, China*
[3]*Department of Engineering and Applied Physics School of Physical Sciences, University of Science and Technology of China, Hefei 230026, China*
[4]*Shenzhen Key Laboratory of Nuclear and Radiation Safety, Institute for Advanced Study in Nuclear Energy & Safety, College of Physics and Optoelectronic Engineering, Shenzhen University, Shenzhen 510640, China*

(Received 1 November 2023; accepted manuscript online 10 April 2024)

Quasi-coherent micro-instabilities is one of the key topics of magnetic confinement fusion. This work focuses on the quasi-coherent spectra of ion temperature gradient (ITG) and trapped-electron-mode instabilities using newly developed far-forward collective scattering measurements within ohmic plasmas in the J-TEXT tokamak. The ITG mode is characterized by frequencies ranging from 30 to 100 kHz and wavenumbers ($k_\theta \rho_s$) less than 0.3. Beyond a critical plasma density threshold, the ITG mode undergoes a bifurcation, which is marked by a reduction in frequency and an enhancement in amplitude. Concurrently, enhancements in ion energy loss and degradation in confinement are observed. This ground-breaking discovery represents the first instance of direct experimental evidence that establishes a clear link between ITG instability and ion thermal transport.

DOI: 10.1088/0256-307X/41/5/055201

The primary mechanism responsible for cross-field particle and heat transport in tokamaks is widely acknowledged to be anomalous transport resulting from micro-instabilities or turbulence.[1–4] As a result, comprehending these micro-instabilities in tokamaks is significantly important for development of future fusion devices. In ohmically heated tokamak plasmas, the ion-temperature-gradient (ITG)-driven drift wave instabilities[5,6] represent one of the most critical micro-instability modes. Theoretical predictions have long indicated that the ITG mode serves as the dominant microscopic turbulence and the primary source of anomalous ion transport within tokamak plasmas.[7–10] However, there is currently limited direct or indirect experimental evidence that conclusively implicates the ITG mode as a specific instability in a tokamak.[11,12] As such, the prominent role of the ITG mode, as anticipated by theory, has yet to be definitively established through experimental means within tokamaks. The challenge to directly distinguish ITG mode in tokamak plasmas is to identify the propagation direction for a specific turbulence. Because the ITG mode usually coexists with the trapped electron mode (TEM) and they have a similar wavelength scale, such that $k_\theta \rho_s < 1$, where k_θ is the poloidal wave number and $\rho_s = \sqrt{m_i T_e}/(Z_i B)$ is the main ion Larmor radius with respect to the main ion sound speed. In early years, using far-infrared (FIR) collective scattering measurements, turbulence with ion features (propagating in the ion diamagnetic drift direction) was observed in saturated ohmic confinement (SOC) plasmas, which was referred to as ITG mode turbulence.[13,14] In recent decades, due to the benefits of the development of reflectometer diagnostics, a particular kind of density fluctuations, called quasi-coherent (QC) modes and concerning the ITG and TEM modes was widely observed in tokamaks.[15–17] The first studies concerning QC modes were performed in the T-10 tokamak, which was reported in Ref. [15]. They found two different QC fluctuations: low-frequency (LF) QC, and high-frequency (HF) QC modes. By comparing with simulations, it was inferred that the LF QC mode was ITG instability, while the HF QC mode was linked with TEM instability. Subsequent studies related to QC modes in TEXTOR and Tore Supra mainly focused on the LF QC modes due to the fact that the HF QC modes were not detected. More recently, a QC mode similar to the LF QC mode in T-10 was also observed on HL-2A and J-TEXT tokamaks by a reflectometer.[18] However, in contrast to Ref. [15], the authors of Refs. [16,18] inferred that LF QC modes were TEM instabilities, although they have quite similar characteristic frequencies of 50–120 kHz and wavenumbers of $k_\theta \rho_s \cong 0.1$–$0.4$. The difference mainly arises from the lack of direct measurement for the propagation direction, which is the key point when judging whether the QC modes are ion or electron modes. In this sense, the FIR collective

*Corresponding author. Email: lijc@szu.edu.cn
© 2024 Chinese Physical Society and IOP Publishing Ltd

scattering measurements[13] have an advantage over reflectometers. However, the collective scattering cannot identify the QC turbulences because it only measures the fluctuation with a particular wavenumber $k_\perp$. Specifically, there is still no direct evidence to affirm the ITG or TEM modes in tokamak experiments.

Most recently, using the newly developed far-forward collective scattering (FCS) measurements,[19] the QC density fluctuation reported in Ref. [18] has also been detected and studied on the Joint-TEXT tokamak (formerly TEXT-U), which is a conventional medium-sized tokamak with a major radius of $R_0 = 1.05$ m and minor radius of $a = 0.25$–0.29 m (set by the silicon-carbide-coated graphite limiter).[20] The FCS measurement is based on the 17-channel three-wave FIR polarimeter-interferometer system (POLARIS),[21] which has the vertical impact parameters $r = -24:3:24$ cm, with $r = R - R_0$. Here, $r < 0$ and $r > 0$ correspond to the high-field side (HFS) and low-field side (LFS), respectively. Additionally, the FCS measures the line-integral electron density fluctuations with the wavenumber in the range of $k_\perp < 1.5\,\mathrm{cm}^{-1}$, where the index $\perp$ means the direction perpendicular to the incident beam.[19] Thus, the maximal detectable poloidal wavenumber varies with the radial position of the measuring chord. It decreases from the center to the edge. It should be noted that all discharges presented here are ohmically heated hydrogen plasmas via gas-puffing fueling. The minor radius a is set at 0.255 m.

The typical density fluctuations spectra measured by FCS are shown in Fig. 1, which are from J-TEXT ohmic discharge with the parameters set as $I_\mathrm{P} = 180$ kA, $B_\mathrm{t} = 2.0$ T, $\bar{n}_{e0} = 3 \times 10^{19}\,\mathrm{m}^{-3}$. The central frequency (885–900 kHz) with large amplitude is the intermediate frequency (IF) signal for measuring the Faraday rotation angle. The two parts beside the IF that are like wings are the collective scattering signals, which are contributed by density fluctuations. There is no scattering signal before discharge, as shown by the dashed line. The frequency difference between the IF (f_0) and scattering signal (f_s) is just the frequency of electron density fluctuation. The scattering spectrum should be symmetric relative to f_0, because the two probe beams are collinear combined. As shown in Fig. 1, the FCS spectra on the $R - R_0 = 18$ cm and $R - R_0 = 0$ cm chords display two peaks at frequencies of $|f_\mathrm{s} - f_0| \cong 70$ and 80 kHz, respectively. The frequency peaks have a broad-band (Δf) about 17 kHz. The characteristic frequency of $\Delta f/f \cong 0.25$ indicates that the density fluctuations have QC features. Additionally, the mid-frequencies of these QC modes have a decreasing tendency with the plasma minor radius. This is consistent with reflectometer observations.[18] Furthermore, the QC mode is absent on the $R - R_0 = -9$ cm chord, while it is noticeable at $R - R_0 = 9$ cm. It shows the clear LFS/HFS asymmetry of the QC modes, which is the same as the QC mode observations on TEXTOR[16] and T-10.[15] Basically, the QC modes are ballooned in the LFS. In fact, for the discharge in Fig. 1, the QC modes can be observed on all the measuring chords from $R - R_0 = 18$ cm to $R - R_0 = -6$ cm. As mentioned above, the wavenumber of density fluctuations measured by FCS is limited as $k_\perp < 1.5\,\mathrm{cm}^{-1}$. Suppose that the electron temperature (T_e) varies from 800 eV to 2 eV while the radial position increases from $r = 0$ cm to $r = 18$ cm, then the normalized wavenumber ($\rho_\mathrm{s} k_\theta$, where $k_\theta = nq/r$ is the poloidal wave number, and $\rho_\mathrm{s} = \sqrt{T_\mathrm{i}/m_\mathrm{i}}/eB$ is the ion Larmor radius, where n is the toroidal number, q is the local safety factor, and B is the local magnetic strength) for the QC mode is estimated as $\rho_\mathrm{s} k_\theta < 0.3$ in the center and $\rho_\mathrm{s} k_\theta < 0.1$ at the edge ($r = 18$ cm).

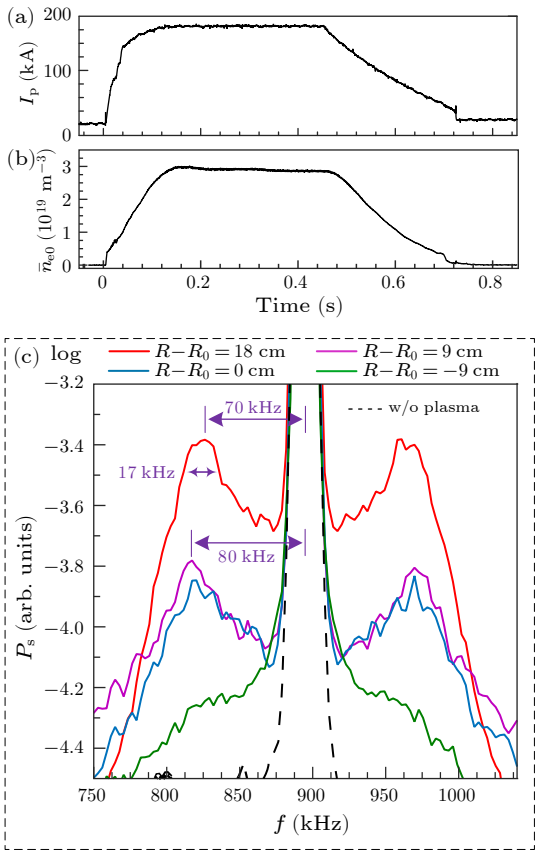

Fig. 1. (a) Plasma current, (b) line-averaged density $\bar{n}_{e0}$, and (c) FCS spectra in the J-TEXT ohmic discharge ($I_\mathrm{P} = 180$ kA, $B_\mathrm{t} = 2.0$ T, $\bar{n}_{e0} = 3 \times 10^{19}\,\mathrm{m}^{-3}$). The QC density fluctuations are seen on chords of $R - R_0 = 18$ cm and $R - R_0 = 0$ cm, but not seen on $R - R_0 = -9$ cm.

According to the collective scattering principle, the heterodyne detection using a twin-frequency source (one acts as a local beam) is available to measure the propagation direction of the density fluctuation wave in the laboratory frame.[22] Of course, it demands that the detector receives the scattering wave from a particular direction. Thus, the frequency shift direction relative to the incident beam corresponds to the propagation direction. For normal far-forward scattering, it is almost impossible to discriminate the propagation direction of density fluctuations, because the scattering waves with positive and negative frequency shifts are symmetric relative to the collection optical path of the detector. However, if the probe beam deviates from the optic axis of the detector collection path, it will be available to identify the propagation direction. For FCS based on POLARIS, which benefits from the probe beam being refracted by the plasma, that

particular deviation exists naturally. Therefore, if the refraction is significant enough, we could discriminate the propagation direction of that QC mode by analyzing the heterodyne signal between local and scattering beams.

The heterodyne FCS spectra mixed by local and scattering beams are plotted in Fig. 2. The IF (2175–2210 kHz) is set to measure the electron density. As shown in Fig. 2(b), the IF amplitude decreases by 25% and 50% at $R - R_0 = 12$ cm and $R - R_0 = -9$ cm, respectively, which results from the refraction of probe beams. As predicted above, the FCS spectra show obvious asymmetry relative to the IF [Fig. 2(a)]. In this discharge, the frequency of the local beam is set to be larger than the probe beam, and the toroidal field is anticlockwise from the top view. Therefore, for the channel at the LFS ($R - R_0 = 12$ cm), the negative frequency shift means that the density fluctuations propagate in the ion diamagnetic direction in the lab frame, while it is opposite for the channel at the HFS ($R - R_0 = -9$ cm). In Fig. 2, both FCS spectra at the LFS and HFS indicate that the QC mode propagates in the ion direction in the lab frame. From calculations with $k_\theta < 1\,\mathrm{cm}^{-1}$ and $f = 70$ kHz, the phase velocity of the QC mode in the lab frame is given as $v_{\mathrm{QC}} > 4.4$ km/s. Considering that the plasma $E \times B$ equilibrium flow usually rotates in the electron direction, the QC velocity is underestimated in the plasma frame. Therefore, it can be affirmed that the QC mode propagates in the ion direction in the plasma frame. Specifically, the QC mode is an ion mode. In addition, the FCS spectrum at $R - R_0 = -9$ cm in Fig. 2 is multiplied by 3. It means that the density fluctuations at the HFS are much smaller than those at the LFS. It should also be noted that the QC mode can be observed within $R - R_0 \leq 18$ cm, but we only presented two for illustrative purposes regarding their propagation direction. Additionally, our measurements are chord-integrated without spatial resolution. However, by comparing measurements from different chords, we can roughly determine their spatial location.

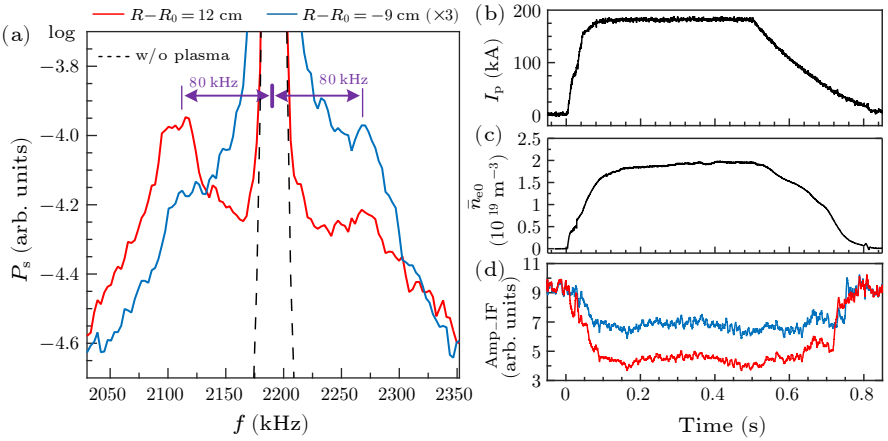

Fig. 2. (a) Heterodyne FCS spectra at $R - R_0 = 12$ cm and $R - R_0 = -9$ cm for J-TEXT ohmic discharge ($I_{\mathrm{P}} = 180$ kA, $B_{\mathrm{t}} = 2.0$ T, $\bar{n}_{\mathrm{e0}} = 2 \times 10^{19}$ m^{-3}). The spectrum at $R - R_0 = -9$ cm is multiplied by 3. (b) Time traces of the plasma current, and (c) line-averaged density $\bar{n}_{\mathrm{e0}}$. (d) Time traces of the amplitudes of the IF in the top panel.

As mentioned above, except for the LF QC mode (70–120 kHz), experiments in the T-10 tokamak found another HF QC mode (150–250 kHz).[15] In fact, in the J-TEXT tokamak, the FCS also measured another QC mode whose characteristic frequency is higher than that in ion QC mode. The heterodyne FCS spectra contain two different QC modes and are shown in Fig. 3. As shown by the spectra in Fig. 2, the ion QC mode (~ 75 kHz) is clearly observed on both chords of $R - R_0 = 12$ cm and $R - R_0 = -3$ cm. However, the different and important point is that another QC mode with characteristic frequency near 170 kHz simultaneously appears in the $R - R_0 = -3$ cm spectrum. The frequency shift direction for the HF QC is opposite to the LF QC. Thus, it can be easily deduced that this HF QC mode propagates in the electron direction in the lab frame. Additionally, the HF QC mode is distinct at the $r = 3$ cm chord but almost disappears at $r = 6$ cm (not shown in Fig. 3). This is mainly because the wavenumber of HF QC mode falls to a value between the measuring limitation of $r = 3$ cm and $r = 6$ cm. Then, its poloidal wavenumber is estimated in the range of $k_\theta \cong 1.4$–$1.5\,\mathrm{cm}^{-1}$. Supposing that $k_\theta = 1.45\,\mathrm{cm}^{-1}$ and $f = 170$ kHz, it gives the HF QC mode phase velocity in the lab frame $v_{\mathrm{HFQC}} \cong 7.3$ km/s in the electron diamagnetic direction. The plasma equilibrium flow poloidal velocity is estimated to be 1–2 km/s, inferred from the carbon ion poloidal velocity measured by a high-resolution spectrometer system.[23] Thus, the HF QC mode is inferred to be electron mode.

All in all, the FCS measurement on J-TEXT has observed two different QC density waves, and they propagate in the ion and electron directions, respectively. The ion and electron QC modes have characteristic frequencies of 50–100 kHz and 150–200 kHz, respectively. Also, the typical wavenumber for ion mode is limited by $\rho_{\mathrm{s}} k_\theta < 0.3$ in the central region and $\rho_{\mathrm{s}} k_\theta < 0.1$ in the edge region, while that for the electron mode is estimated as $0.15 < \rho_{\mathrm{s}} k_\theta < 0.3$. For ohmic L-mode tokamak plasmas, the most unstable micro-instabilities with long wavelengths ($\rho_{\mathrm{s}} k_\theta < 1$) are predicted to be ITG and TEM

modes. Also, the normalized wavenumber for the two QC modes is close to the theoretical predictions.[24] When considering the propagation direction, it is reasonable to conclude that the ion QC mode is ITG instability and the electron QC mode is TEM instability. In addition, we should note that the TEM mode is difficult to measure, because its wavenumber is close to the limitation of the FCS measurement on J-TEXT. Thus, here we mainly study the ITG mode in the following.

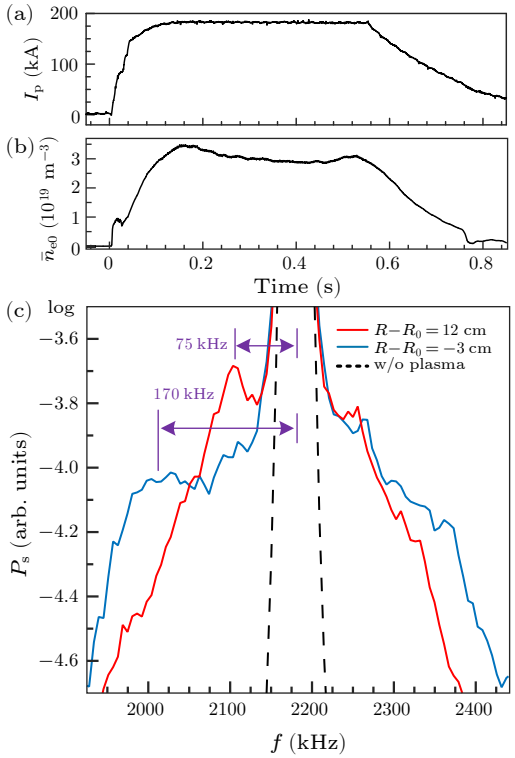

Fig. 3. Time traces of the plasma current (a) and the line-averaged density $\bar{n}_{e0}$ (b). (c) Heterodyne FCS spectra at $r = 12$ cm and $r = -3$ cm for J-TEXT ohmic discharge. The QC ion mode and another QC electron mode are observed.

As it is suggested that the stability of ITG mode is strongly related to plasma density and confinement saturation in tokamaks, we have studied the behavior of ITG mode during density rising. For the discharge using continual gas puffing to raise the density in one shot, the FCS spectrum ($r = 12$ cm) evolution with central averaged electron density ($\bar{n}_{e0}$) is shown in Fig. 4. The discharge parameters are $I_P = 180$ kA, $B_t = 2.0$ T, and the density climbs from 1.5×10^{19} m^{-3} to 4.5×10^{19} m^{-3}. It is necessary to note that the FCS spectra in Fig. 4 are normalized by density ($P_{FCS}/\bar{n}_{e0}$). According to the behavior of the ITG modes, this discharge can be divided into three density regimes. In the low-density (LD) range ($\bar{n}_{e0} < 2 \times 10^{19}$ m^{-3}), the ITG mode is too weak to be observed, as shown by the spectrum for $\bar{n}_{e0} = 1.8$. In the medium-density (MD) range ($\bar{n}_{e0} = 2$—3.5×10^{19} m^{-3}), the ITG mode is noticeable and enhances slowly with the density increase. Meanwhile, its characteristic frequency almost remains constant. In the high-density (HD) range ($\bar{n}_{e0} > 3.5 \times 10^{19}$ m^{-3}), the amplitude of ITG mode increases substantially with density, and its characteristic frequency decreases simultaneously. It is important to note that in Figs. 1 and 4, the far-forward collective scattering (FFCS) measurements are from the intermediate frequency (IF) signal between two probe beams, which measures the line-integral Faraday rotation angle. Conversely, in Figs. 2 and 3, the FFCS measurements are from the intermediate frequency (IF) signal between the local beam and one probe beam, which measures the line-integral electron density. It is important to note that the propagation direction of density fluctuation is only measurable by the IF signal between the local and probe beams. For a more detailed explanation, one can refer to our previously published theoretical and diagnostic article.[25]

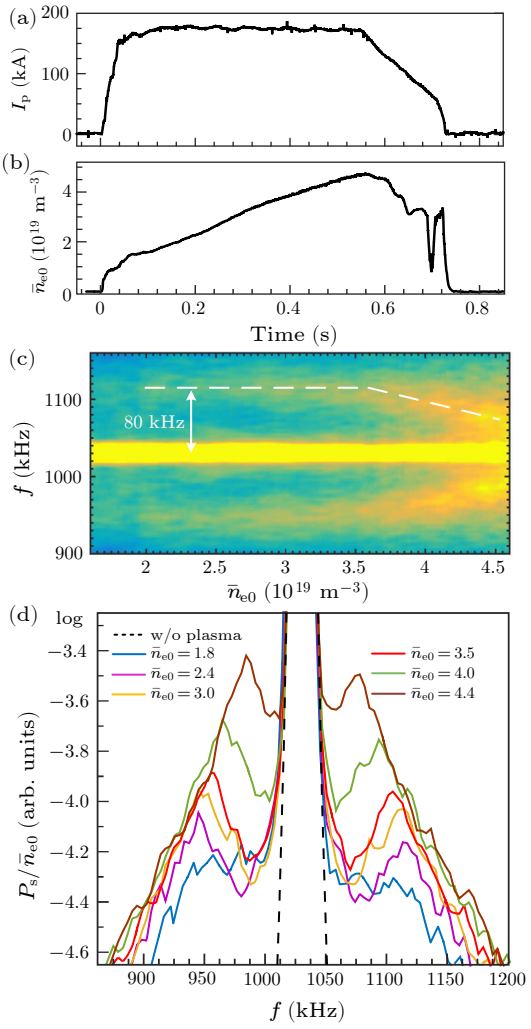

Fig. 4. Evolution of (a) the plasma current, (b) the line-averaged density $\bar{n}_{e0}$ and [(c), (d)] the normalized FCS spectra ($R - R_0 = 12$ cm) with the central averaged electron density ($\bar{n}_{e0}$) for a density ramp-up discharge. The discharge parameters are $I_P = 180$ kA, $B_t = 2.0$ T.

As shown in Fig. 4, during the HD regime, the normalized fluctuation power ($P_s/\bar{n}_{e0}$) for ITG mode has trebled, and its central frequency decreases from 8 kHz to 40 kHz. In a word, the ITG mode behavior has two bifurcation points. The first point is the appearance of ITG mode, and the corresponding critical density is $\sim 2 \times 10^{19}$ m^{-3}.

The second point is the abrupt amplitude increase and frequency decrease for ITG mode, and the corresponding critical density is $\sim 3.5 \times 10^{19}\,\mathrm{m}^{-3}$. It is believed that the SOC regime is related to the bifurcation behavior of ITG mode. According to the empirical scaling by Shimomura *et al.*,[26] the critical density for SOC is predicted as $n_{\mathrm{e}}^{c} = I_{\mathrm{p}}\mu_0\sqrt{A_{\mathrm{i}}}/(2\sqrt{2}\pi a^2) \cong 3.9 \times 10^{19}\,\mathrm{m}^{-3}$. It is much closer to the second bifurcation point. The stored energy of ions and the density peaking factor can also serve as indicators of confinement performance. As depicted in Fig. 5(c), during later stages, both the density profile peaking factor and ion energy exhibit flattening trends, suggesting a transition from the linear ohmic confinement to the SOC. Moreover, it should be noted that the ITG is not necessarily dominant only at low densities; it is merely more observable under such conditions. We concurrently observe both the ITG and TEM, indicating that the ITG does not exert sole dominance.

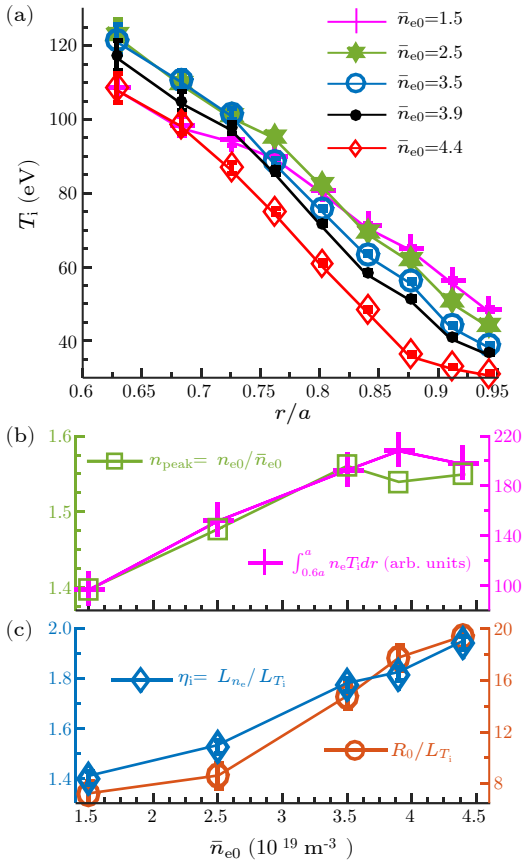

Fig. 5. Dependences of the ion temperature profile (a), density profile peaking factor and ion energy in the edge region (b), $\eta_{\mathrm{i}} = L_n/L_T$ and R_0/L_T at $r/a = 0.7$ (c) on the central line-averaged electron density.

Furthermore, we have studied the ion temperature profile and the ITG critical parameters $\eta_{\mathrm{i}} = L_n/L_{T_{\mathrm{i}}}$ for the slab branch and $R_0/L_{T_{\mathrm{i}}}$ for the toroidal branch. The ion temperature profile at the edge ($r > 0.6a$) is given by a high-resolution spectrometer system, and the plasma density profile is obtained by POLARIS.[27] As shown in Fig. 5(c), both η_{i} and $R_0/L_{T_{\mathrm{i}}}$ (at $r = 0.7a \sim 18\,\mathrm{cm}$) increase with the density climbing. This is why ITG mode enhances with density. The correlation between the ITG mode amplitude and η_{i} has been affirmed by experiments in CLM.[28] Also, the critical value of η_{i} for ITG mode occurrence (where $\bar{n}_{e0} \approx 2 \times 10^{19}\,\mathrm{m}^{-3}$) is about 1.5. This is consistent with the theoretical prediction. In addition, the ion temperature [Fig. 5(a)] in the core region ($r < 0.6a$) shows an abrupt decline after the density exceeds $3.5 \times 10^{19}\,\mathrm{m}^{-3}$. Meanwhile, the density profile peaking factor ($n_{e0}/\bar{n}_{e0}$) and the ion energy in the region ($r > 0.6a$) both reach maxima, as indicated by Fig. 5(b). This implies the enhancement of ion energy losses and global confinement degradation. The critical density $\bar{n}_{e0} \cong 3.5 \times 10^{19}\,\mathrm{m}^{-3}$ is highly consistent with the threshold of the abrupt enhancement for ITG mode. For the plasma discharge parameter in Fig. 5(c), at high densities, the electron cyclotron emission (ECE) diagnostic does not meet the optical thickness conditions; as a result, the temperature profile measurements are unavailable. Consequently, the density profile information is encapsulated in Fig. 4(b), where the density peak is derived from the density profile. This peak precisely provides the information we seek. Therefore, we have opted not to present the radial profiles of electron density. Moreover, the quantity R_0/L_{ne} in Fig. 5(c) is defined as $R_0/L_{T_{\mathrm{i}}}$ divided by η_{i}. It is important to note that J-TEXT currently lacks a direct diagnostic system for measuring stored energy, such as a diamagnetic probe. However, within the context of ohmic heating and high-density scenarios, the stored energy of electrons and ions is essentially equal. Therefore, using the stored energy of ions in our study can effectively represent the overall stored energy. Additionally, it is worth mentioning that turbulence primarily resides within the region where the normalized minor radius is between 0.6 and 0.95. Profiles below 0.6 are relatively flat, indicating that the ITG dominates beyond $R - R_0 = 18\,\mathrm{cm}$. This suggests that the provided distribution of stored energy here represents the predominant region of turbulence activity, and turbulence in the core region does not significantly affect the overall confinement.

In summary, we have provided experimental confirmation of the existence of ion temperature gradient (ITG) and trapped electron mode (TEM) instabilities with quasi-coherent spectra in toroidal plasma.[29–31] These findings were obtained via far-forward collective scattering measurements conducted in the J-TEXT tokamak. Notably, the ITG mode exhibits bifurcation behavior upon surpassing a critical plasma density threshold, resulting in a significant enhancement. Coinciding with this phenomenon, we observed a substantial increase in ion energy loss and a degradation in global confinement. These observations furnish direct experimental evidence for ion thermal transport driven by the ITG mode.

Acknowledgements. This work was partially supported by the National Natural Science Foundation of China (Grant Nos. 0204131240 and 11575067), the Shenzhen Municipal Collaborative Innovation Technology Program-International Science and Technology (S&T) Cooperation Project (Grant No. GJHZ20220913142609017), and the "Fourteenth Five-Year Plan" Basic Technological Research Project (Grant No. JSZL2022XXXX001).

References

[1] Garbet X, Mantica P, Angioni C *et al.* 2004 *Plasma Phys. Control. Fusion* **46** B557
[2] Bourdelle C 2005 *Plasma Phys. Control. Fusion* **47** A317
[3] Wan B and EAST team 2020 *Chin. Phys. Lett.* **37** 045202
[4] Hu W, Feng H Y, and Zhang W L 2019 *Chin. Phys. Lett.* **36** 085201
[5] Cowley S C, Kulsrud R M, and Sudan R 1991 *Phys. Fluids B* **3** 2767
[6] Horton W 1999 *Rev. Mod. Phys.* **71** 735
[7] Dimits A M, Williams T J, Byers J A, and Cohen B I 1996 *Phys. Rev. Lett.* **77** 71
[8] Horton W, Lindberg D, Kim J Y, Dong J Q, Hammett G W, Scott S D, Zarnstorff M C, and Hamaguchi S 1992 *Phys. Fluids B* **4** 953
[9] Li J, Xu J Q, Qu Y R, Lin Z, Dong J Q, Peng X D, and Li J Q 2023 *Nucl. Fusion* **63** 096005
[10] Li J C, Dong J Q, and Liu S F 2020 *Plasma Sci. Technol.* **22** 055101
[11] Brower D L, Peebles W A, Kim S K, Luhmann Jr N C, Tang W M, and Phillips P E 1987 *Phys. Rev. Lett.* **59** 48
[12] Rettig C L, Staebler G M, Rhodes T L, Doyle E J, Peebles W A, and Burrell K H 2001 *Plasma Phys. Control. Fusion* **43** 1273
[13] Brower D L, Redi M H, Tang W M *et al.* 1989 *Nucl. Fusion* **29** 1247
[14] Rettig C L, Rhodes T L, Leboeuf J N, Peebles W A, Doyle E J, Staebler G M, Burrell K H, and Moyer R A 2001 *Phys. Plasmas* **8** 2232
[15] Vershkov V A, Shelukhin D A, Soldatov S V *et al.* 2005 *Nucl. Fusion* **45** S203
[16] Arnichand H, Sabot R, Hacquin S *et al.* 2014 *Nucl. Fusion* **54** 123017
[17] Krämer-Flecken A, Dreval V, Soldatov S *et al.* 2004 *Nucl. Fusion* **44** 1143
[18] Zhong W L, Shi Z B, Yang Z J, Xiao G L, Yang Z C, Zhang B Y, Shi P W, Du H R, Pan X M, Zhou R B, Wan L H, Zou X L, Xu M, Duan X R, Liu Y, Zhuang G, HL-2A Team, and J-TEXT Team 2016 *Phys. Plasmas* **23** 060702
[19] Shi P, Chen J, Gao L, Liu Y, Liu H, Zhou Y N, and Zhuang G 2016 *Rev. Sci. Instrum.* **87** 11E110
[20] Zhuang G, Pan Y, Hu X W, Wang Z J, Ding Y H, Zhang M, Gao L, Zhang X Q, Yang Z J, Yu K X, Gentle K W, Huang H, and J-TEXT Team 2011 *Nucl. Fusion* **51** 094020
[21] Zhuang G, Liu Y, Chen J, Gao L, Li Q, Xiong C Y, Shi P, and Zhou Y N 2016 *J. Instrum.* **11** C02026
[22] Brower D L, Peebles W A, Kim S K, and Luhmann Jr N C 1988 *Rev. Sci. Instrum.* **59** 1559
[23] Cheng Z F, Luo J, Wang Z J, Zhang Z P, Zhang X L, Hou S Y, Cheng C, Li Z, and Zhuang G 2014 *Rev. Sci. Instrum.* **85** 11E423
[24] Weiland J and Nordman H 1991 *Nucl. Fusion* **31** 390
[25] Shi P, Qiu Q S, Zhuang G, Gao L, Zhou Y N, and Zhou C X 2018 *Rev. Sci. Instrum.* **89** 10C110
[26] Shimomura Y, Suzuki N, Sugihara M, Tsuda T, Odajima K, and Tsunematsu T 1985 *Japanese Atomic Energy Research Institute Report* JAERI-M-85-080
[27] Chen J, Zhuang G, Jian X, Li Q, Liu Y, Gao L, and Wang Z J 2014 *Rev. Sci. Instrum.* **85** 103501
[28] Sen A K, Chen J, and Mauel M 1991 *Phys. Rev. Lett.* **66** 429
[29] Shen Y C, Lyu B, Wang F D, Shi Y J, Wu B, Li Y Y, Fu J, and Wan B N 2016 *Chin. Phys. Lett.* **33** 065205
[30] Li J C, Dong J Q, Ji X Q, and Hu Y J 2021 *Chin. Phys. B* **30** 075203
[31] Li J C, Gong X Y, Dong J Q, Wang J, and Yin L 2016 *Chin. Phys. B* **25** 045201